

# Impact of Excitation Frequency and Fill Levels on Fuel Sloshing in Automotive Tanks

Rajamani Rajagounder ✉ – Jayakrishnan Nampoothiri

Department of Production Engineering, PSG College of Technology, India

✉ rajamani.vrr@gmail.com

**Abstract** Fuel sloshing in modern automotive fuel tanks is analyzed in this study to provide a better understanding of fuel system performance. The behaviour of sloshing waves was investigated under varying excitation frequencies and fuel fill levels using both experimental and numerical methods. A sinusoidal motion was applied to the fuel tank along its transverse axis, and the resulting wave profiles were captured using a digital camera setup. Numerical simulations were conducted using the volume of fluid (VOF) model and a user-defined function (UDF) in ANSYS Fluent to predict the sloshing wave profiles. The study reveals distinct wave patterns depending on the excitation frequency. Standing and traveling waves were observed at 0.5 Hz and 0.6 Hz, while multiple traveling waves with wave collisions occurred at 0.7 Hz. Additionally, increasing the fuel fill level (from 25 % to 60 % of tank height) significantly enhanced the damping of sloshing wave oscillations. Regression equations were developed to quantify the relationship between excitation frequency, fill level, and sloshing wave amplitude. These findings may contribute to the design of fuel tanks that mitigate sloshing effects and enhance overall vehicle performance.

**Keywords** liquid sloshing, fuel tank, finite volume analysis, visualization, wave frequency

## Highlights

- Visualized free-surface fuel motion using numerical and experimental methods
- Identified wave behaviour at 0.7 Hz with strong standing and traveling wave formation
- Found increased fill levels enhance damping and accelerate wave decay
- Developed regression models linking frequency and fill level to wave amplitude

## 1 INTRODUCTION

Fuel sloshing in automotive tanks poses significant challenges, particularly in controlling wave behaviour under varying frequencies and fill levels [1]. Various studies have aimed to understand the dynamic sloshing phenomena and mitigate its effects using different modelling techniques, experimental methods, and tank modifications. One of the foundational approaches to studying sloshing was provided by Faltinsen [2], who developed a nonlinear numerical method for two-dimensional flow, offering crucial insights into the fluid motion inside a tank under excitation. Expanding further on this, Dongming and Pengzhi [3] employed a three-dimensional model to examine sloshing dynamics, illustrating the complexities introduced by additional spatial dimensions.

Recent advancements have focused on combining computational methods with experimental validation to enhance prediction accuracy. The volume of fluid (VOF) method, commonly used in numerical simulations, has been applied effectively to analyse sloshing behaviour under various conditions. Zhao et al. [4] utilized this approach to explore nonlinear sloshing in rectangular tanks under forced excitation, uncovering the development of standing and traveling waves at different frequencies. Similarly, Jin and Lin [5] analysed the viscous effects on sloshing, demonstrating the importance of accounting for fluid properties when modelling dynamic sloshing behaviour. Qiu et al. [6] and Liu et al. [7] used the VOF method to study liquid sloshing, finding that higher fill levels and first-order natural frequency intensify sloshing forces. Elahi et al. [8] and Topçuand Kılıç [9] also developed VOF-based numerical models for sloshing simulation.

Experimental approaches complement numerical methods by validating theoretical predictions. For instance, Rajamani et al. [10] conducted an experimental study to capture free surface wave profiles

in a fuel tank subjected to uniform acceleration, and the resulting wave profiles were compared with numerical results. Furthermore, Babar et al. [11] explored the coupled Eulerian-Lagrangian (CEL) method for simulating multiphysics events in automobiles, bridging the gap between computational models and real-world applications.

The incorporation of baffles has emerged as an effective method to dampen sloshing. Frandsen [12] examined sloshing in tanks with an annular baffle, which showed significant suppression of wave amplitude. Similarly, Wang et al. [13] demonstrated that multiple rigid annular baffles in cylindrical tanks reduce sloshing effects by altering the flow dynamics and dissipating energy. Park et al. [14] conducted an experimental study on liquid sloshing in a rectangular tank with both rigid and flexible baffles, detailing the behaviour of free surfaces at different fill levels and excitation frequencies. Wang et al. [15] investigated the impact of different baffle configurations on liquid sloshing in a partially filled cylindrical tank mounted on a truck. The findings indicate that the introduction of baffles enhances the fundamental sloshing frequency and decreases the likelihood of resonance phenomena in tank vehicles. These findings have led to practical applications in automotive fuel tanks, whereby baffles and partitions are used to control the liquid motion and enhance vehicle stability. Moreover, parametric studies have revealed the influence of various factors, such as fill level, excitation frequency, and tank geometry, on sloshing behaviour. Gurusamy et al. [16] explored shallow water tanks' sloshing dynamics, focusing on the hydraulic jumps formed during wave interactions, providing insights into wave-breaking mechanisms under certain frequencies. Sanapala et al. [17] performed numerical simulations on baffled rectangular tanks, highlighting the relationship between baffle height and sloshing suppression.

Despite significant advancements in understanding fuel sloshing dynamics, challenges remain in accurately predicting sloshing

behaviour under varying operating conditions and improving mitigation techniques. Current models often overlook the interplay between multiple factors affecting sloshing, leading to suboptimal designs. Therefore, this study made an attempt on a comprehensive approach that combines experimental validation with numerical simulations to explore the effects of excitation frequency and fill levels on sloshing in automotive fuel tanks. By integrating innovative tank modifications and computational techniques, this research aims to enhance prediction accuracy and provide new insights for optimizing fuel tank designs. The combined use of numerical simulations and experimental methods has significantly advanced the understanding of fuel sloshing in automotive tanks. These studies not only help mitigate the risks associated with sloshing but also contribute to optimizing tank designs for improved vehicle safety and performance.

## 2 METHODS & MATERIALS

### 2.1 Numerical Simulation

This study uses the VOF method to simulate liquid sloshing, implemented in ANSYS FLUENT (V16.2). The governing equations for incompressible fluid motion in the tank are described by the continuity equation in Eq. (1) and the momentum equation in Eq. (2),

$$\nabla \cdot V = 0, \tag{1}$$

$$\rho \left( \frac{\partial V}{\partial t} + V \cdot \nabla V \right) = -\nabla P + \rho g + \mu \nabla^2 V. \tag{2}$$

An open channel flow boundary condition is applied, utilizing a first-order upwind scheme for discretizing convective terms. The geometric reconstruction scheme determines the cell values at the liquid-air interface, represented by volume fractions ( $\lambda$ ), where '0' indicates air and '1' indicates liquid. The volume fraction equation is expressed as Eq. (3),

$$\frac{\partial \lambda}{\partial t} + \nabla \cdot (\lambda u) = 0. \tag{3}$$

The presence of air or liquid in each cell is calculated using Eq. (4),

$$\sum_{j=1}^n \lambda_j = 1, \tag{4}$$

where  $n=2$  for two phases fluid flow problems and  $\lambda_j$  is the volume fraction of  $j^{\text{th}}$  phase.

The volume fraction equation is solved using explicit time formulation. In a two-phase flow problem, the density ( $\rho$ ) of liquid in each cell is determined using Eq. (5),

$$\rho = \lambda_2 \rho_2 + (1 - \lambda_2) \rho_1. \tag{5}$$

The stability of the numerical solution is controlled by the time step ( $\Delta t$ ) and element size ( $\Delta x$ ) which is expressed in terms of Courant number ( $C$ ) given in Eq. (6),

$$C = u \frac{\Delta t}{\Delta x}. \tag{6}$$

The  $C$  value is maintained at less than 1 to control the stability of the numerical solution. Also, to analyze the effects of random vibrations on the fuel tank, sinusoidal motion along the horizontal  $x$ -axis is applied, represented by Eq. (7),

$$u = X_0 \omega \cos \omega t. \tag{7}$$

In ANSYS Fluent software, a user defined function (UDF) with the macro DEFINE\_CG\_MOTION is used to set translation motion at the tank's centre of gravity. The quiescent liquid is assigned zero velocity and ambient pressure at the surface, while gravitational

acceleration is applied along a vertical axis. Implicit body force treatment enhances the solution convergence. Surface tension effects are neglected, and the tank wall is modelled as a rigid structure.

A grid independence study is conducted with three different mesh sizes. The total number of cells 90,561, 110,441, and 156,492 yielding free surface wave amplitudes of 9.43 mm, 10.27 mm, and 10.31 mm, respectively. Based on accuracy, computational time, and memory usage, numerical simulations are performed using 110,441 quadrilateral cells.

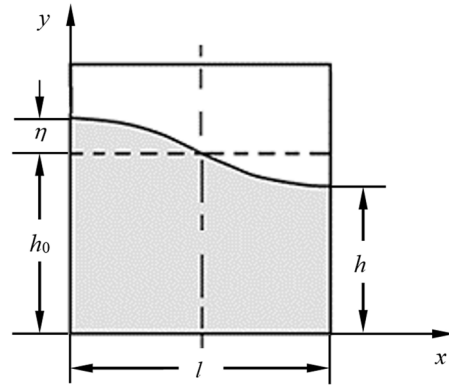


Fig. 1. Sloshing wave in a tank

Fig. 1 shows the sloshing wave in a tank and its amplitude. The natural frequency of the sloshing wave depends upon the fill level ( $h_0$ ) and tank length ( $l$ ). The motion of sloshing wave under gravity field can be expressed using Eq. (8) [18],

$$v = \frac{\partial \eta}{\partial t} + u \frac{\partial \eta}{\partial x}, \tag{8}$$

where  $\partial \eta / \partial x$  represents the slope of the free surface.

The magnitude of free surface from mean liquid level ' $\eta$ ' can be calculated using linear analytical solution obtained by Faltinsen [2]. When the tank is subjected to sinusoidal motion, the magnitude of the free surface is given in Eq. (9). The amplitude of the sloshing waves obtained from numerical simulations and experimental studies is compared with the result of Eq. (9).

$$\eta = \frac{1}{g} \sum_{n=0}^{\infty} \sin \left\{ \frac{(2n+1)\pi}{l} x \right\} \cosh \left\{ \frac{(2n+1)\pi}{l} h_0 \right\} \left[ -A_n \omega_n \sin \omega_n t - C_n \omega \sin \omega t \right] - \frac{1}{g} A \omega x \sin \omega t. \tag{9}$$

where,  $n = 0, 1, 2, 3, \dots$

$$\omega_n^2 = g \frac{(2n+1)\pi}{2l} \tanh h \left\{ \frac{(2n+1)\pi}{2l} h_0 \right\},$$

$$C_n = \frac{\omega K_n}{\omega_n^2 - \omega^2}, \quad A_n = -C_n - \frac{K_n}{\omega}, \quad \text{and}$$

$$K_n = \frac{\omega A}{\cosh \left\{ \frac{(2n+1)\pi}{l} h_0 \right\}} \frac{4}{l} \left[ \frac{l}{(2n+1)\pi} \right]^2 (-1)^n.$$

The fundamental frequency ( $f_n$ ) of the sloshing waves in a partially filled tank is given in Eq. (10),

$$f_n = \frac{1}{2\pi} \sqrt{\frac{g\pi}{l} \tanh \left( \frac{\pi h_0}{l} \right)}. \tag{10}$$

With  $g = 9.81 \text{ m/s}^2$ , tank length of 370 mm and fill level of 70 mm, the fundamental frequency of the wave is 1.06 Hz. At this

frequency, violent sloshing will occur and the sloshing wave motion becomes highly turbulent. To avoid this, the tank is excited below the first natural frequency of the sloshing wave.

### 2.2 Experimental Studies

The experimental setup consists of a reciprocating table with a slider-crank mechanism, a direct current (DC) motor, a transparent composite fuel tank, a speed control unit, and a digital camera, as illustrated in Fig. 2a. The computer aided design (CAD) model of the bottom portion of the tank is shown in Fig. 2b, while the spatial dimensions of the tank are detailed in Fig. 2c. Sinusoidal motion is applied using a slider crank with a crank radius of 25 mm, and the frequency is adjusted by varying the motor speed.

A transparent fuel tank is fabricated and the front portion of the tank is covered with an acrylic sheet for better visibility of the sloshing waves. Water mixed with a colouring agent serves as the working liquid. A Redlake's Motion Pro™ CMOS PCI camera with a maximum shutter speed of 10,000 fps (frames per seconds) records the sloshing waves at 60 fps. Captured images are converted to grayscale, and edge detection is employed to identify the liquid-air interface.

When using gasoline for experiments, the fuel tank must be sealed to prevent fuel vapor leakage. Therefore, water is utilized in this study. Kinematic and dynamic similarities in free surface flow are maintained using similitude relations based on Reynolds number ( $Re$ ) and Froude number ( $Fr$ ), as proposed by Abramson and Ransleben [19].

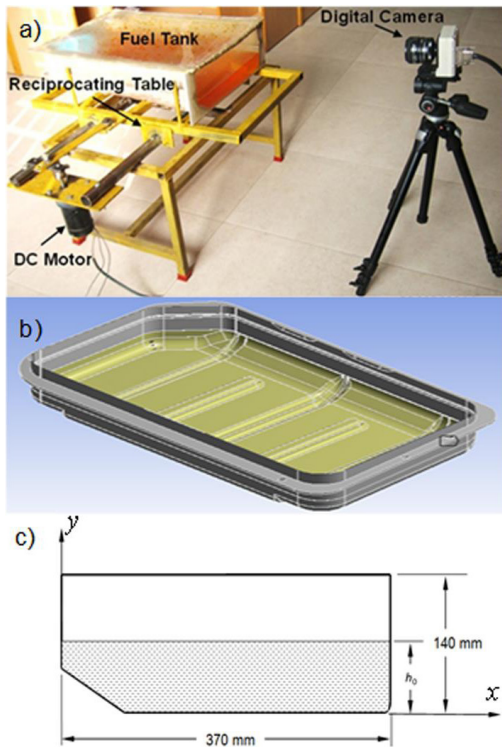


Fig. 2. a) Experimental setup, b) CAD model of a fuel tank, and c) spatial dimensions of a fuel tank

The similitude relation for free surface wave problem is given in Eq. (11)

$$\frac{Fl^2}{\rho l^4} = \phi \left( \frac{at^2}{l}, \frac{h}{l}, \frac{X_0}{l}, \frac{\rho l^2}{\mu t} \right) \tag{11}$$

From Eq. (11), the non-dimensional number for the amplitude of the sloshing wave ( $H^*$ ) and time ( $T^*$ ) can be expressed as Eqs. (12) and (13)

$$H^* = \frac{h}{l}, \tag{12}$$

$$T^* = t \sqrt{\frac{a}{l}} \quad (\text{or}) \quad T^* = \omega_n \cdot t. \tag{13}$$

In this study, the results obtained from numerical simulations and experimental studies are presented using the non-dimensional numbers  $H^*$  and  $T^*$ .

### 3 RESULTS AND DISCUSSION

The free surface motion of liquid in an automotive fuel tank is analysed for different excitation frequencies such as 0.5 Hz, 0.6 Hz and 0.7 Hz and fill levels ( $h_0/H$ ) of 0.25, 0.33, 0.5 and 0.6. The formation of sloshing waves and the amplitude of the waves are predicted numerically and compared with the experimental results.

#### 3.1 The Effect of Excitation Frequency on Sloshing Wave Motion

The formation of sloshing waves in a partially filled container depends on factors such as tank shape, liquid level, fluid properties, and excitation parameters [20]. This study investigates sloshing wave behaviour at various oscillation frequencies, specifically at 0.5 Hz, 0.6 Hz, and 0.7 Hz, comparing numerical results with experimental findings in a tank filled to 50 % of its height. Fig. 3a shows the initial position of the free surface of a liquid. At 0.5 Hz, Fig. 3 shows the evolution of sloshing waves, starting with a standing wave that transitions to a traveling waves (Figs. 3b and c), with numerical simulations closely aligning with experimental results (Figs. 3d to f). At 0.6 Hz, the initial standing wave (Figs. 4a and b) evolves into a traveling wave (Figs. 4c), with noticeable differences between numerical and experimental wave patterns emerging after 1.6 seconds (Figs. 4c and f), indicating a phase lag in oscillation magnitude (Fig. 6b).

At 0.7 Hz, Fig. 5 depicts the formation of a standing wave, which subsequently transforms into multiple traveling waves (Figs. 5a and b). The occurrence of two traveling waves colliding results in a superimposed wave (Figs. 5c and e), characteristic of bore wave patterns. These patterns are evident in the corresponding experimental results shown in Figs. 5g to h. The comparative analysis across frequencies highlights the complexities of wave dynamics in sloshing scenarios, emphasizing the relevance of numerical simulations in predicting wave behaviour.

The findings provide insights into sloshing wave dynamics across different oscillation frequencies. The transition from standing to traveling waves highlights the impact of frequency on wave propagation, with higher frequencies facilitating more dynamic interactions, such as collisions and superimpositions. The phase lag observed at 0.6 Hz indicates potential discrepancies between numerical simulations and experimental results, likely due to simplified model assumptions and the neglect of surface tension effects, which can significantly influence real-world wave behaviour. Nevertheless, the alignment of numerical and experimental results at lower frequencies suggests that the VOF approach effectively captures fundamental sloshing dynamics, establishing its utility in predicting sloshing behaviour in fuel tanks.

Fig. 6a compares the temporal evolution of the non-dimensional amplitude of the free surface of liquid between numerical simulations and experimental studies, when the tank undergoes sinusoidal motion at 0.5 Hz. At this frequency, the maximum non-dimensional

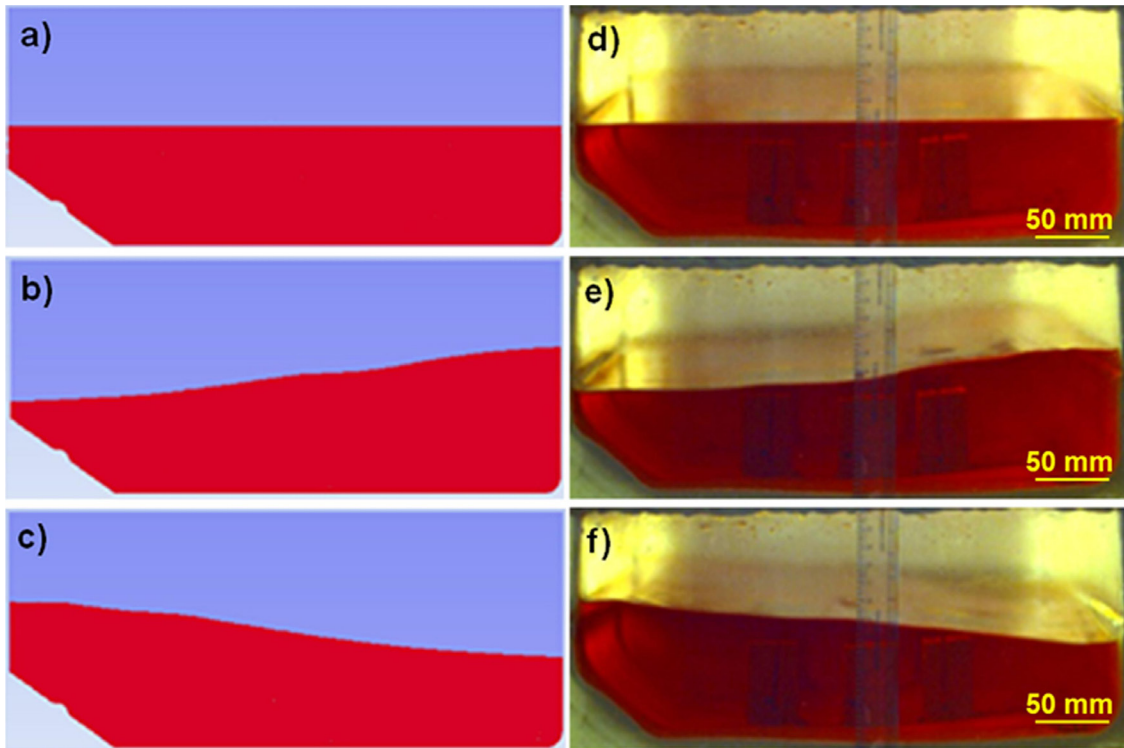


Fig. 3. Slushing wave profiles at 0.5 Hz: numerical results; a) water level at  $t = 0$  s, b) standing wave at  $t = 0.8$  s, c) standing wave at  $t = 1.5$  s; and experimental results: d) water level at  $t = 0$  s, e) standing wave at  $t = 0.8$  s, f) standing wave at  $t = 1.5$  s

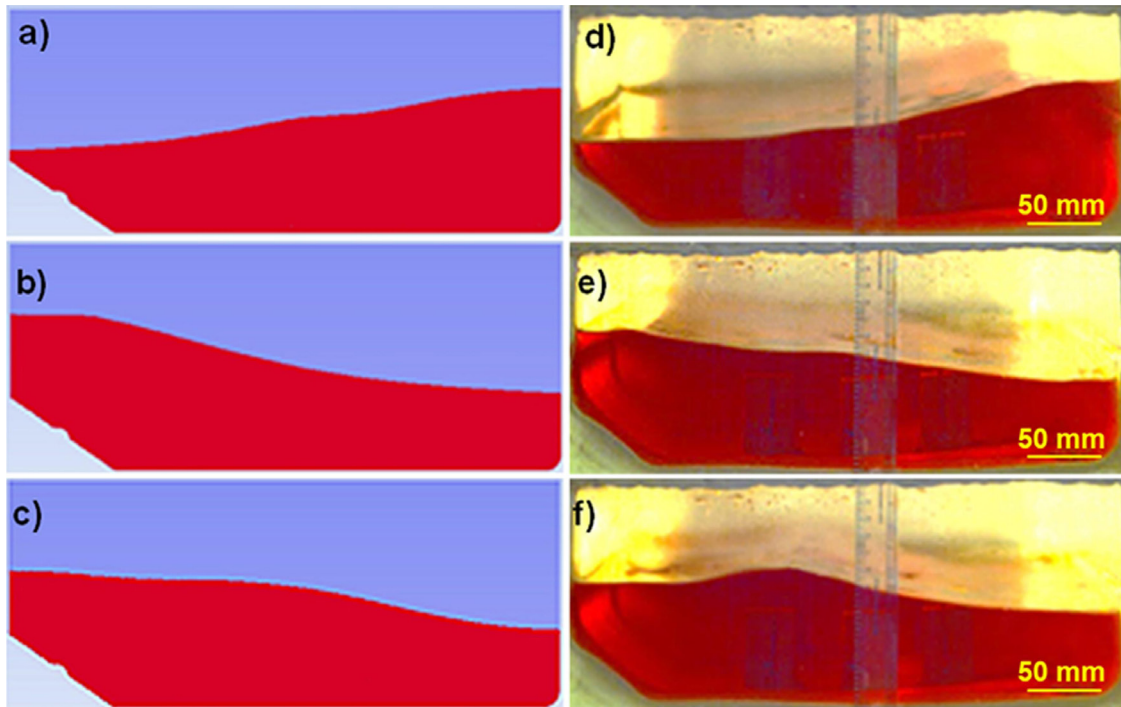


Fig. 4. Slushing wave profiles at 0.6 Hz: numerical results; a) standing wave at  $t = 0.8$  s, b) standing wave at  $t = 1.4$  s, c) travelling wave at  $t = 1.6$  s; and experimental results: d) standing wave at  $t = 0.8$  s, e) standing wave at  $t = 1.4$  s, and f) travelling wave at  $t = 1.6$  s

amplitude of the sloshing wave ( $H^*$ ) is 0.246 as showed by simulations and 0.233 determined from experiments, showing good agreement. However, the experimental results exhibit secondary wave crest-troughs that are absent in the numerical model.

Similarly, Fig. 6b presents the comparison at an oscillatory frequency of 0.6 Hz. The simulated maximum  $H^*$  values are 0.250,

while experimental value reach 0.246. Initially, the sloshing wave amplitudes align well, but subsequent cycles reveal additional crest-troughs in the experimental data, which are not predicted by the numerical simulations.

Fig. 6c illustrates the temporal evolution of  $H^*$  at 0.7 Hz. Here, the simulated maximum  $H^*$  values are 0.352 and 0.364 based on

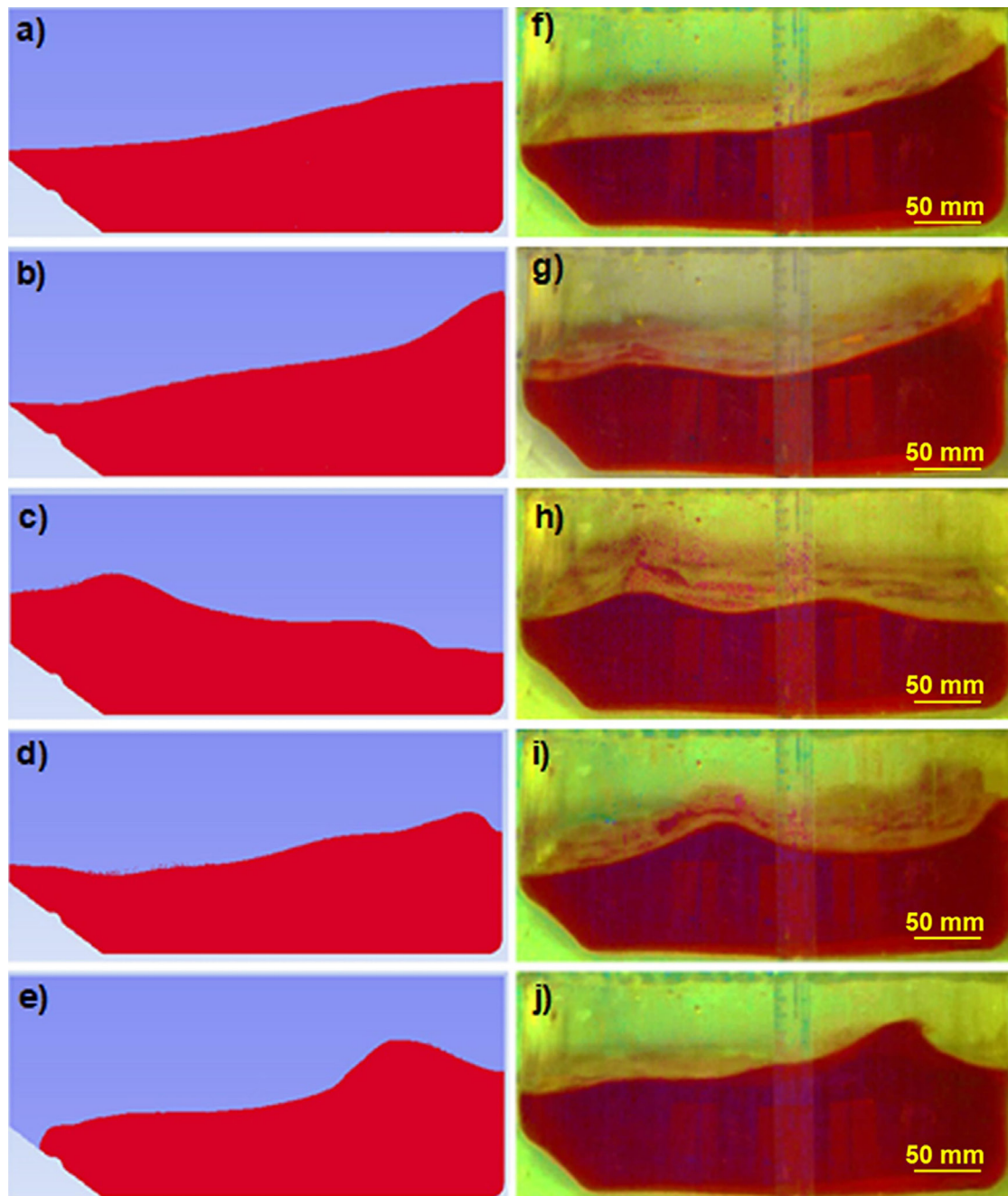


Fig. 5. Slashing wave profiles at 0.7 Hz: numerical results; a) standing wave at  $t = 0.7$  s, and traveling waves at b)  $t = 1.9$  s, c)  $t = 2.5$  s, d)  $t = 3.2$  s, e)  $t = 3.6$  s; and experimental results: f) standing wave at  $t = 0.7$  s and traveling waves at g)  $t = 1.9$  s, h)  $t = 2.5$  s, i)  $t = 3.2$  s, j)  $t = 3.6$  s

experiments. A significant deviation in sloshing wave motion arises in the numerical results due to the formation and interaction of multiple traveling waves.

The maximum amplitude of sloshing waves ( $H^*$ ) from numerical simulations and experimental studies is validated against the analytical solution provided by Faltinsen [2]. Fig. 7 depicts the relationship between the maximum non-dimensional amplitude ( $H^*$ ) and the frequency ratio ( $\omega/\omega_n$ ), showing an increase in amplitude with higher excitation frequencies. Regression equations derived from standard curve fitting techniques further illustrate this relationship, as represented in Fig. 7.

At 0.5 Hz and 0.6 Hz, the numerical and experimental results align closely with the analytical solution. However, at 0.7 Hz,

notable deviations between numerical and experimental findings are observed, highlighting limitations in the numerical model at higher frequencies. As the tank motion frequency approaches the natural frequency of the sloshing wave, the liquid's free surface experiences violent sloshing. Standing waves transition into traveling waves, leading to wave collisions that create turbulence. This turbulence results in deviations between the amplitudes of sloshing waves obtained from numerical and experimental analyzes compared to the analytical model.

### 3.2 The Effect of Fill Level on Amplitude of Sloshing Wave

The effect of fill levels on the amplitude of sloshing waves is analyzed using sinusoidal motion applied to the tank, as governed by

Eq. (7). An excitation amplitude of 25 mm and a frequency of 0.5 Hz are applied. The analysis considers various liquid levels: 25 %, 33 %, 50 %, and 60 % of the tank height. As the liquid level increases, the mass of the liquid absorbing the disturbances also increases, resulting in an increased fundamental frequency of the sloshing waves and a decrease in wave amplitude.

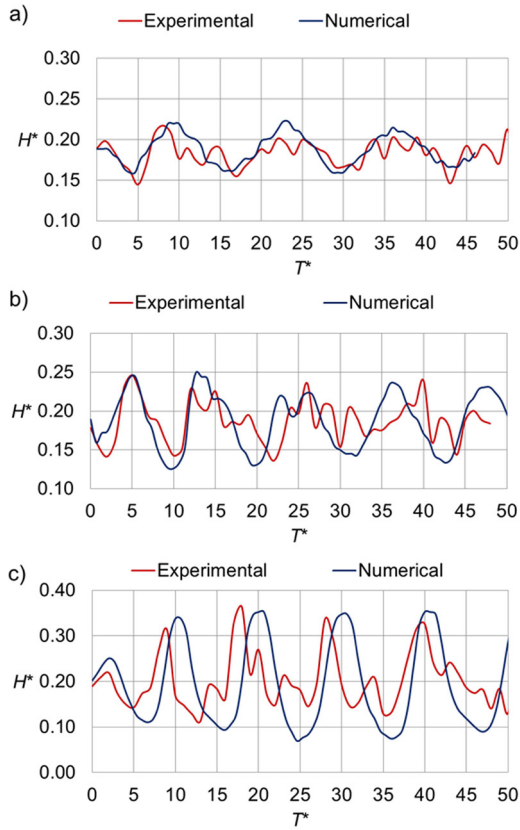


Fig. 6. Non-dimensional amplitude of sloshing wave for: a)  $f = 0.5$  Hz, b)  $f = 0.6$  Hz, and c)  $f = 0.7$  Hz

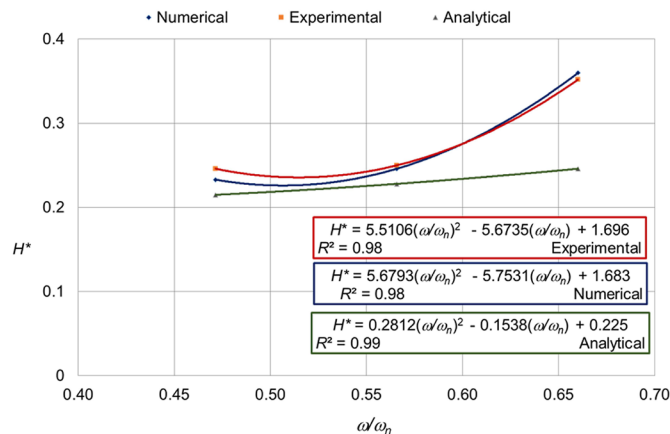


Fig. 7. Maximum amplitude of the sloshing wave versus frequency ratio

Fig. 8 compares the amplitude of sloshing wave motion at different liquid levels, highlighting changes in the wavelength of free surface oscillations as the liquid level increases. Fig. 9 illustrates the relationship between the non-dimensional amplitude of the sloshing wave ( $\eta/l$ ) and the liquid level ratio ( $h_0/H$ ). The study shows that the magnitude of the sloshing wave decreases with higher liquid levels. At a fill level of 50 %, experimental results deviate by a maximum of 18 % from numerical simulations. The formation of multiple

waves and turbulence in the liquid flow contributes to variations in numerical simulation results. A regression equation is formulated to estimate the amplitude of the sloshing wave at specified fill levels.

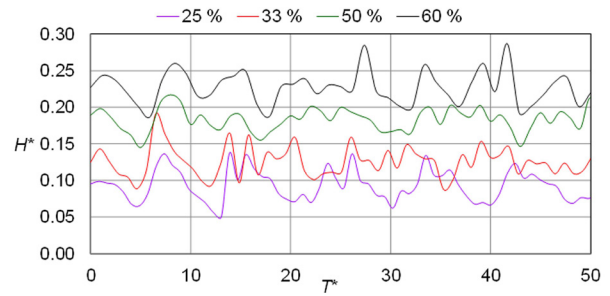


Fig. 8. Amplitude of the sloshing wave motion at the different fill levels

### 3.3 The Effect of Fill Level on the Damping of Sloshing Wave Oscillations

The damping factor of a sloshing wave in a closed container is influenced by the liquid's viscosity, tank size, and fill level.

This study examines the effect of fill level on the damping of free surface wave oscillations by applying an acceleration of 1.6 m/s<sup>2</sup> to the tank for 2 seconds, after which the tank is free from external excitation. The sloshing wave then oscillates under free vibration, and the decay rate of wave oscillations is recorded for fill levels of 25 %, 33 %, 50 %, and 60 % of the tank height. The amplitudes of the sloshing waves for these fill levels are presented in Fig. 10a.

The hydrodynamic damping of the free surface wave is calculated using the logarithmic decrement method adopted from Ibrahim [21]. The logarithmic decrement ( $\delta$ ) is determined using Eq. (14).

$$\delta = \frac{1}{n} \ln \left[ \frac{x_r}{x_{n+r}} \right], \tag{14}$$

where  $x_r$  is the amplitude of the sloshing wave in any reference cycle and  $x_{n+r}$  is the amplitude of the sloshing wave after completing 'n' number of cycles.

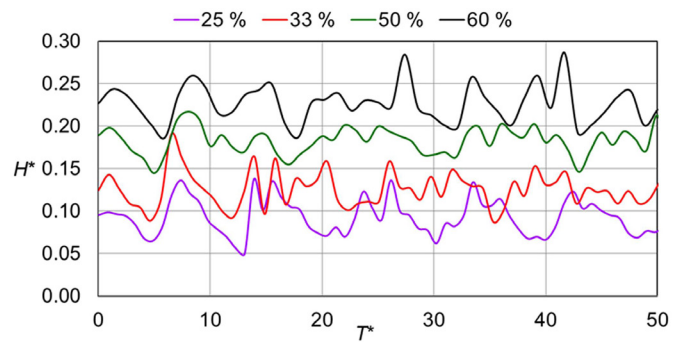


Fig. 9. Maximum amplitude of the sloshing wave at various fill levels

Fig. 10b illustrates the effect of fill level on the hydrodynamic damping of a sloshing wave. It is observed that damping increases with higher fill levels due to the increased liquid mass, which absorbs the kinetic energy of the sloshing waves. A regression equation is formulated to represent the relationship between the liquid fill level and changes in damping, minimizing sloshing effects.

The sloshing behaviour of fuel is analyzed by applying excitation motion along the transverse axis of the tank. Future work could extend this research by incorporating violent sloshing and combined excitation along both the longitudinal and transverse axes of the fuel tank. This regression equation can be used to predict the damping of

sloshing wave oscillations at fill levels within the range adopted in this study.

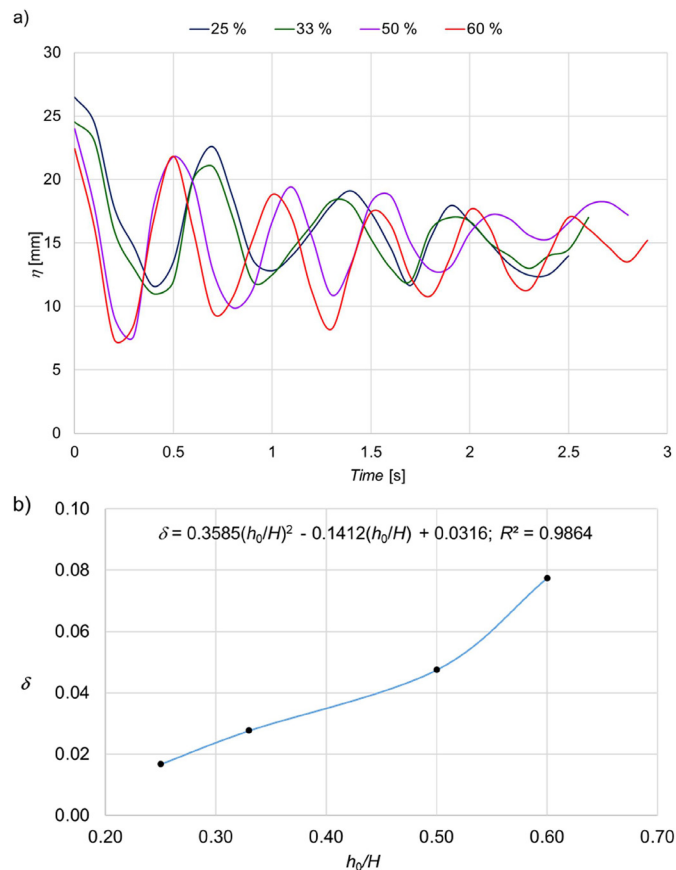


Fig. 10. a) Decay of the amplitude of the sloshing wave under free vibration, and b) damping of the sloshing wave oscillations

## 4 CONCLUSIONS

This study analyzes liquid sloshing in a fuel tank at various oscillation frequencies and fill levels through numerical simulations and experimental studies using the VOF approach. The key findings are as follows:

The applied oscillation frequency significantly affects the formation of sloshing waves. At frequencies of 0.5 Hz and 0.6 Hz, a standing wave forms and subsequently transitions into a traveling wave. At 0.7 Hz, the standing wave evolves into multiple traveling waves, leading to wave collisions that create turbulence in the liquid motion.

The effect of fill levels on the amplitude of sloshing waves is examined with tanks filled to 25 %, 33 %, 50 %, and 60 % of their height. As the fill level increases, the logarithmic decrement also increases, causing the oscillation of the free surface wave to decay more rapidly.

Regression equations are developed to represent the effects of tank motion frequency and fill levels on sloshing wave amplitude.

This study provides valuable insights for automotive engineers to visualize and understand free surface wave behaviour, aiding in the design of fuel tanks that minimize sloshing effects. Future research can expand on this work by exploring violent sloshing and combined excitations along both the longitudinal and transverse axes of the fuel tank.

## Nomenclature

$A$  velocity of the tank, [m s<sup>-1</sup>]  
 $a$  acceleration of the tank, [m s<sup>-2</sup>]  
 $C$  courant number, [-]  
 $F$  force exerted by the liquid on tank wall, [N]  
 $F_r$  Froude number, [-]  
 $f_n$  natural frequency, [Hz]  
 $g$  acceleration due to gravity, [m s<sup>-2</sup>]  
 $H$  tank height, [m]  
 $H^*$  non-dimensional free surface elevation, [-]  
 $h_0$  fill level, [m]  
 $h$  amplitude of free surface oscillations, [m]  
 $l$  tank length, [m]  
 $P$  fluid pressure, [N m<sup>-2</sup>]  
 $Re$  Reynolds number, [-]  
 $T^*$  non dimensional number derived from time  $t$  [-]  
 $t$  time, [s]  
 $u$  velocity component along the  $x$  axis, [m s<sup>-1</sup>]  
 $V$  velocity of fluid, [m s<sup>-1</sup>]  
 $v$  velocity component along the  $y$  axis, [m s<sup>-1</sup>]  
 $X_0$  displacement of the tank, [m]  
 $x$  distance from origin, [m]  
 $\Delta t$  time step, [s]  
 $\Delta x$  grid length, [m]  
 $\lambda$  volume fraction, [-]  
 $\eta$  elevation of free surface from mean liquid level, [m]  
 $\mu$  dynamic viscosity of the fluid, [N s m<sup>-2</sup>]  
 $\rho$  density of the fluid, [kg m<sup>-3</sup>]  
 $\omega$  excitation frequency, [rad s<sup>-1</sup>]  
 $\omega_n$  natural angular frequency, [rad s<sup>-1</sup>]

## References

- [1] aus der Wiesche, S. Computational slosh dynamics: theory and industrial application. *Comput Mech* 30 374-387 (2003) DOI:10.1007/s00466-003-0413-8
- [2] Faltinsen, O.M. A numerical nonlinear method of sloshing in tanks with two-dimensional flow. *J Ship Res* 22 193-202 (1978) DOI:10.5957/jsr.1978.22.3.193
- [3] Liu, D., Lin, P. A numerical study of three-dimensional liquid sloshing in tanks. *J Comput Phys* 227 3921-3939 (2008) DOI:10.1016/j.jcp.2007.12.006
- [4] Zhao, D., Hu, Z., Chen, G., Lim, S., Wang, S. Nonlinear sloshing in rectangular tanks under forced excitation. *Int J Nav Arch Ocean* 10 545-565 (2018) DOI:10.1016/j.ijnaoe.2017.10.005
- [5] Jin, X., Lin, P. Viscous effects on liquid sloshing under external excitations. *Ocean Eng* 171 695-707 (2019) DOI:10.1016/j.oceaneng.2018.10.024
- [6] Qiu, Y., Bai, M., Liu, Y., Lei, G., Liu, Z. Effect of liquid filling level on sloshing hydrodynamic characteristic under the first natural frequency. *J Energy Storage* 55 105452 (2022) DOI:10.1016/j.est.2022.105452
- [7] Liu, Z., Yuan, K., Liu, Y., Andersson, M., Li, Y. Fluid sloshing hydrodynamics in a cryogenic fuel storage tank under different order natural frequencies. *J Energy Storage* 52 104830 (2022) DOI:10.1016/j.est.2022.104830
- [8] Elahi, R., Passandideh-Fard, M., Javanshir, A. Simulation of liquid sloshing in 2D containers using the volume of fluid method. *Ocean Eng* 96 226-244 (2015) DOI:10.1016/j.oceaneng.2014.12.022
- [9] Topçu, E.E., Kılıç, E. A numerical investigation of sloshing in a 3D prismatic tank with various baffle types, filling rates, input amplitudes and liquid materials. *Appl Sci* 13 2474 (2023) DOI:10.3390/app13042474
- [10] Rajamani, R., Guru Vignesh M., Prakasan K., A study of liquid sloshing in an automotive fuel tank under uniform acceleration. *Eng J* 20 71-85 (2016) DOI:10.4186/ej.2016.20.1.71
- [11] Babar, R.T., Pakalapati, V., Katkar, V. Application of CEL method for simulation of multiphysics events in automobiles. *SAE J Mater Manuf* 4 969-979 (2011) DOI:10.4271/2011-01-0793
- [12] Frandsen, J.B. Sloshing motions in excited tanks. *J Comput Phys* 196 53-87 (2004) DOI:10.1016/j.jcp.2003.10.031
- [13] Wang, J., Wang, C., Liu, J. Sloshing reduction in a pitching circular cylindrical container by multiple rigid annular baffles. *Ocean Eng* 171 241-249 (2019) DOI:10.1016/j.oceaneng.2018.11.013

- [14] Park, T., Park, C.-J., Lee, J., Kim, Y. Experimental observation on violent sloshing flows inside rectangular tank with flexible baffles. *Appl Ocean Res* 154104307 (2025) DOI:10.1016/j.apor.2024.104307
- [15] Wang, Q., Qi, W., Zheng, G., Xu, W., Yu, H. Liquid sloshing in a tank vehicle: A numerical and experimental investigation with baffle configurations. *Measurement* 234 114806 (2024) DOI:10.1016/j.measurement.2024.114806
- [16] Gurusamy, S., Sanapala, V.S., Kumar, D., Patnaik, B.S.V. Sloshing dynamics of shallow water tanks: Modal characteristics of hydraulic jumps. *Journal Fluids Struct* 104 103322 (2021) DOI:10.1016/j.jfluidstructs.2021.103322
- [17] Sanapala, V.S., Rajkumar, M., Velusamy, K., Patnaik, B.S.V. Numerical simulation of parametric liquid sloshing in a horizontally baffled rectangular container. *J Fluid Struct* 76 229-250 (2018) DOI:10.1016/j.jfluidstructs.2017.10.001
- [18] Milne-Thomson, L.M. *Theoretical Hydrodynamics*. Macmillan Education, London (1968)
- [19] Abramson, H.N., Martin, R., Ransleben, G.E. (1958). *Application of Similitude Theory to the Problem of Fuel Sloshing in Rigid Tanks*. Southwest Research Institute, San Antonio
- [20] Chen, Y.G., Djidjeli, K., Price, W.G. Numerical simulation of liquid sloshing phenomena in partially filled containers. *Comput Fluids* 38 830-842, (2009) DOI:10.1016/j.compfluid.2008.09.003
- [21] Ibrahim, R.A. (2005). *Liquid Sloshing Dynamics: Theory and Applications*. Cambridge University Press, Cambridge, DOI:10.1017/CB09780511536656

**Acknowledgement** The authors thank the management of PSG College of Technology, Coimbatore, TamilNadu, India, for providing the necessary facilities to carry out this research.

Received 2024-10-23, revised 2025-02-27, accepted 2025-03-19  
as Original Scientific Paper.

**Data availability** All data that support the findings of this study are included within the article.

**Author contributions** Rajamani Rajagounder: conceptualization, formal analysis, investigation, methodology, resources and writing – original draft; Jayakrishnan Nampoothiri: writing – review & editing, data curation, validation and visualization.

**AI-Assisted writing** AI-based tools were employed solely to enhance the readability and grammatical accuracy of the manuscript.

## Vpliv vzbujalne frekvence in nivoja napolnjenosti na pljuskanje goriva v avtomobilskih rezervoarjih

**Povzetek** Študija obravnava analizo procesa pljuskanja goriva v sodobnih avtomobilskih rezervoarjih z namenom boljšega razumevanja delovanja gorivnega sistema. Obnašanje valovanja pri pljuskanju je bilo obravnavano pri različnih vzbujalnih frekvencah in nivojih napolnjenosti rezervoarja, in sicer z eksperimentalnimi ter numeričnimi metodami. Rezervoar za gorivo je bil vzdolž prečne osi izpostavljen sinusnemu gibanju, profili valov pa so bili zajeti z digitalno kamero. Numerične simulacije so bile izvedene z uporabo aproksimacije proste površine (metoda VOF) in uporabniško definirane funkcije (UDF) v programu ANSYS Fluent. Študija je pokazala različne oblike valovanja glede na vzbujalno frekvenco. Pri frekvencah 0,5 Hz in 0,6 Hz so bili opaženi stoječi in potujoči valovi, pri 0,7 Hz pa več potujočih valov z medsebojnimi trki. Poleg tega je povečanje nivoja napolnjenosti (z 25 % na 60 % višine rezervoarja) bistveno izboljšalo dušenje oscilacij valov. Razvite so bile regresijske enačbe za kvantitativno opredelitev odnosa med vzbujalno frekvenco, nivojem napolnjenosti in amplitudo valov. Ti izsledki lahko prispevajo k načrtovanju rezervoarjev, ki zmanjšujejo učinke pljuskanja in izboljšajo delovanje vozila.

**Ključne besede** pljuskanje tekočine, rezervoar za gorivo, analiza končnih volumnov, vizualizacija, frekvenca valovanja